

# THE KINETICS OF FORMATION OF TWISTED INTRAMOLECULAR CHARGE TRANSFER (TICT) STATES IN *p*-SUBSTITUTED DIALKYLANILINES: CONSEQUENCES OF CONICAL INTERSECTIONS ALONG THE REACTION COORDINATE<sup>†</sup>

WOLFGANG RETTIG and GÜNTER WERMUTH

*Iwan N. Stranski Institute for Physical and Theoretical Chemistry, Technical University of Berlin, Strasse des 17 Juni 112, D-1000 Berlin 12 (F.R.G.)*

(Received January 2, 1985)

## Summary

The dual fluorescence spectra of a series of dialkylaminobenzonitriles and dialkylaminobenzoesters measured at room and low temperature in polar and non-polar solvents are compared. The esters always show a higher ratio of long-wavelength to short-wavelength fluorescence. This ratio strongly depends on the type of dialkylamino substituent. In non-polar solvents it is highest for the compound with the lowest donor ionization potential ( $D \equiv 2,5$ -dimethylpyrrolidino). The fluorescence spectra show clear evidence of dual fluorescence (twisted intramolecular charge transfer (TICT) emission) even for the corresponding nitrile in alkane solvents. This is rationalized by invoking thermodynamic control of TICT state formation. In the case of polar solvents the order of the rate constants for TICT state formation is changed such that for rotating parts of similar size it correlates with the initial Franck-Condon twist angle, indicating kinetic control. Low temperature quantum yield measurements and direct laser kinetic data show that in *n*-butyl chloride at low temperatures the rate of formation of the TICT states of the esters is a factor of 2 - 13 greater than that of the nitriles. This is ascribed to the presence of a conical intersection along the reaction coordinate in the case of the nitriles. Microviscosity theory is used to discuss some effects which depend on the size of the dialkylamino substituents and on the nature of the solvent in terms of the available free volume for rotation.

---

## 1. Introduction

Since the initial discovery by Lippert *et al.* [1] of the dual fluorescence of *p*-dimethylaminobenzonitrile (DMABN) in polar solvents a number of

---

<sup>†</sup>Dedicated to Professor Dr. Dietrich Schulte-Frohlinde on the occasion of his 60th birthday.

other substituted dialkylanilines with dual fluorescence have been found. Replacing the cyano group by aldehyde, ketone [2] or sulfone [3] substituents leads to a similar dual fluorescence which, in the case of ester substituents, is clearly visible in non-polar solvents [4]. DMABN in non-polar solvents emits a very small fraction of the long-wavelength fluorescence band  $F_A$  [5] which is generally associated with the twisted intramolecular charge transfer (TICT) excited state [6]. In this paper the ester- and cyano-substituted dialkylanilines are compared in more detail.

One of the main differences between these two groups of compounds is the difference in the correlation of the excited states. The initially populated locally excited  $B^*$  state of the approximately planar molecule which emits the short-wavelength fluorescence  $F_B$  correlates with two different states for the twisted geometry. These are the emitting  $A^*$  (TICT) state in the case of esters and the second singlet excited state ( ${}^1L_b$  type) in the case of nitriles [7]. An excited state crossing is required to reach the TICT state in nitriles. This is a consequence of the different natures of the precursors of the TICT states: the  $B^*$  state is of the  ${}^1L_a$  type in the case of the esters but of the  ${}^1L_b$  type in the case of the nitriles, as can be seen by their different fluorescence polarization and radiative decay rates  $k_f$  [7]. A smooth transition between these two extremes is possible by means of vibronic coupling effects as is shown by the solvent-polarity-dependent fluorescence rate constant of *N*-ethylindoline-5-carboxylic acid ethyl ester, which is a planar model compound for the ester series [8].

The consequence of the difference in the correlation of the excited states is an increase in the relative TICT fluorescence yield for the esters compared with that for the nitriles under identical conditions [4]. This is due to the faster rate of TICT state formation for the esters [9]. The esters show appreciable TICT fluorescence even in saturated hydrocarbon solvents [4]. This is because the transition  $B^* \rightarrow$  TICT is thermoneutral or slightly exothermic for esters in saturated hydrocarbons, whereas it is endothermic for nitriles [5] and therefore the population of the TICT state is smaller.

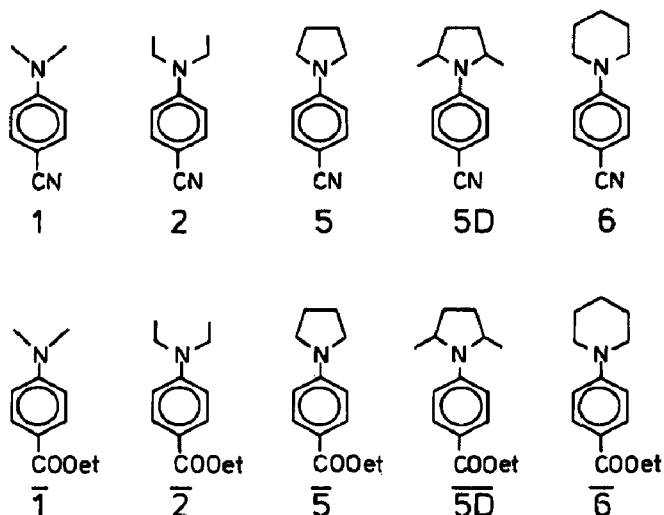
It has been shown for the nitrile series that the relative rate  $\bar{k}$  of TICT state formation strongly depends on the type of dialkylamino substituent [10 - 12]. The main factors governing  $\bar{k}$  for a given solvent are (i) the twist angle in the ground state [11, 12], (ii) the size of the dialkylamino group (two additional methyl substituents on a piperidino ring reduce the rate constant by a factor of 1.8 [11]) and (iii) the flexibility of the dialkylamino group (the TICT state of a piperidino-substituted benzonitrile is formed much faster than that of a pyrrolidino-substituted benzonitrile because relaxation along part of the reaction coordinate is possible due to its intramolecular flexibility [10, 11]).

The dual fluorescence properties and associated rate constants of (i) the esters in polar and non-polar solvents and (ii) esters and nitriles in polar solvents are compared in detail in order to gain a deeper insight into the mechanism. It will be shown that vibronic coupling effects are of prime importance, and that microscopic solvent cavities also play a major role.

Additional evidence is provided for the occurrence of dual fluorescence from nitriles in non-polar solvents. This fact, together with the similar behaviour observed for the relative intensity of the long-wavelength fluorescence band in corresponding nitriles and esters, is difficult to accommodate in a model involving specific solute-solvent complexes [13 - 15].

## 2. Experimental details

The following dialkylaminobenzoic acid nitriles and esters were investigated:



Compounds 5, 5D and 6 [10] and  $\bar{5}$ ,  $\bar{5D}$  and  $\bar{6}$  [16] were synthesized via the nucleophilic substitution of 4-fluorobenzoic acid ester or nitrile [17]. The new compounds  $\bar{5}$ ,  $\bar{5D}$  and  $\bar{6}$  were identified by their nuclear magnetic resonance and mass spectra [16]. The melting points of  $\bar{5}$  and  $\bar{6}$  were at 376 - 377 K and 352 - 353 K respectively;  $\bar{5D}$  was a colourless oil at room temperature. All crystalline compounds were recrystallized several times and finally vacuum sublimed.  $\bar{5D}$  was chromatographed on silica gel using 4:1 petrol ether-diethyl ether as the eluent. The nitrile data were taken from ref. 10. The solvents were purified by chromatography and fractional distillation as described for *n*-butyl chloride in ref. 7 and for the alkanes in ref. 4.

Quantum-corrected fluorescence spectra of solutions with concentrations of about  $2 \times 10^{-6}$  M were measured on a FICA 55 MK II spectrofluorometer (bandwidth, 7.5 nm). The low temperature quantum yields  $\Phi_A$  were determined using *p*-terphenyl in cyclohexane as the standard ( $\Phi_f = 0.93$ ), and the values were corrected for changes of refractive index and

absorbance with temperature [5, 7]. These  $\Phi_A$  values and the ratio  $\Phi_p/\Phi_f$  of phosphorescence to fluorescence quantum yields at 77 K [7, 18] were used to determine the ratio  $k_{Af}/(k_{Af} + k_{A^{\circ}})$  according to the equation

$$\left(\frac{k_{Af}}{k_{A^{\circ}} + k_{Af}}\right)^{-1} = \Phi_A^{-1} - \left(\frac{\Phi_A}{\Phi_B}\right)^{-1} \left(1 + \frac{\Phi_p}{\Phi_f}\right) \quad (1)$$

which was derived from eqns. (2) - (4) (Section 4.2) by setting  $k_B^{\circ} = k_{ISC}$  (77 K). The resulting rate constants  $\bar{k}$  are given in Table 4 (section 4.2).

The fluorescence decay times were determined using a mode-locked neodymium glass laser system as described in ref. 11. Within the accuracy of the detection system (fast photodiode and storage oscilloscope), the decays observed in the low temperature range were single exponential.

### 3. Results

The fluorescence properties of two selected pairs of nitriles and esters in a non-polar and a polar solvent are shown in Figs. 1 and 2. The ester always shows a higher ratio of long-wavelength (TICT) to short-wavelength ( $F_B$ ) fluorescence. The relative TICT yield for 5D and  $\bar{5D}$  is strongly increased compared with 1 and  $\bar{1}$ . Thus  $\bar{5D}$  shows predominant TICT fluorescence with a maximum near 380 nm even in a non-polar hydrocarbon solvent. The dimethylpyrrolidino substituent in 5D and  $\bar{5D}$  is so favourable for TICT formation at room temperature that even the corresponding nitrile 5D shows readily visible dual emission in saturated hydrocarbon solvents. Its fluorescence band in *n*-hexane is appreciably broadened (Fig. 2) to a half-width  $\Delta\nu_{1/2}$  of about  $3800 \text{ cm}^{-1}$  compared with the values of  $3300 - 3400 \text{ cm}^{-1}$  obtained for 5 and 1 in *n*-hexane and is equal to that of  $\bar{1}$  in *n*-hexane (Fig. 1). This agrees with recent findings of Visser *et al.* [15] for  $\bar{1}$  and is clear evidence that the emission of TICT fluorescence in saturated hydrocarbon solvents is not limited to esters but can also occur for nitriles, although to a lesser extent [5].

Figure 3 shows the ratio  $\Phi_A/\Phi_B$  of the long-wavelength to the short-wavelength fluorescence quantum yields as a function of inverse temperature for the nitrile and ester series in the medium polar solvent *n*-butyl chloride. Above the temperature  $T_{\max}$ , where this ratio reaches a maximum, dynamic equilibrium  $B^* \rightleftharpoons A^*$  is established during the excited state lifetime; only the irreversible transition  $B^* \rightarrow A^*$  takes place below  $T_{\max}$  [2, 6, 19].

The data for  $T_{\max}$  and the maximum value of  $\Phi_A/\Phi_B$  reached at  $T_{\max}$  are given in Table 1 together with the  $\Phi_A/\Phi_B$  values at 150 K which is in the low temperature irreversible regime, *i.e.* below  $T_{\max}$ , for all compounds studied. The main features to be noted are as follows: (i) the  $T_{\max}$  values are roughly equal for the nitrile and ester series but depend strongly on the dialkylamino substituent; (ii) the maximum value of  $\Phi_A/\Phi_B$  is reached for compounds 2 ( $\bar{2}$ ) and 5D ( $\bar{5D}$ ), and the minimum value is reached for com-

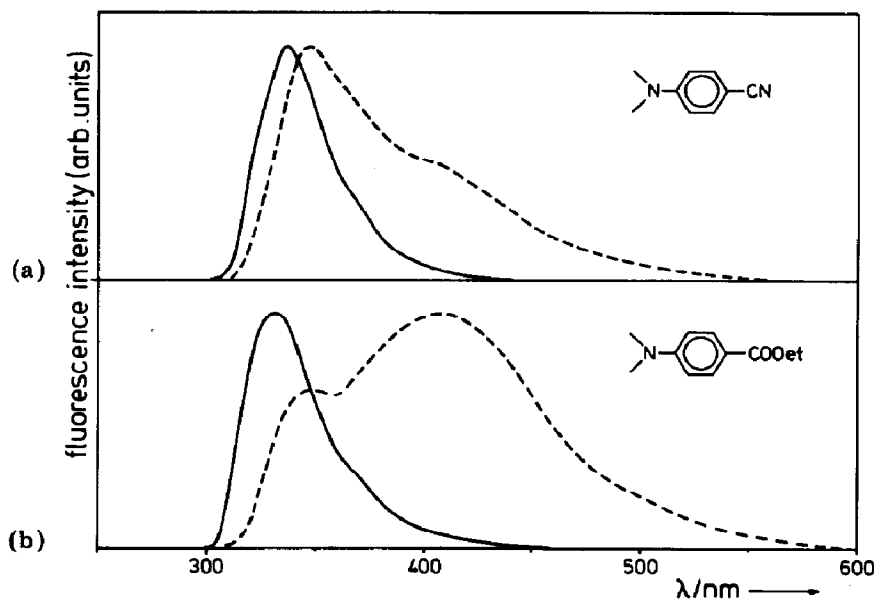


Fig. 1. Fluorescence spectra of (a) compound 1 and (b) compound  $\bar{1}$  in *n*-hexane (—) and *n*-butyl chloride (---) at room temperature.

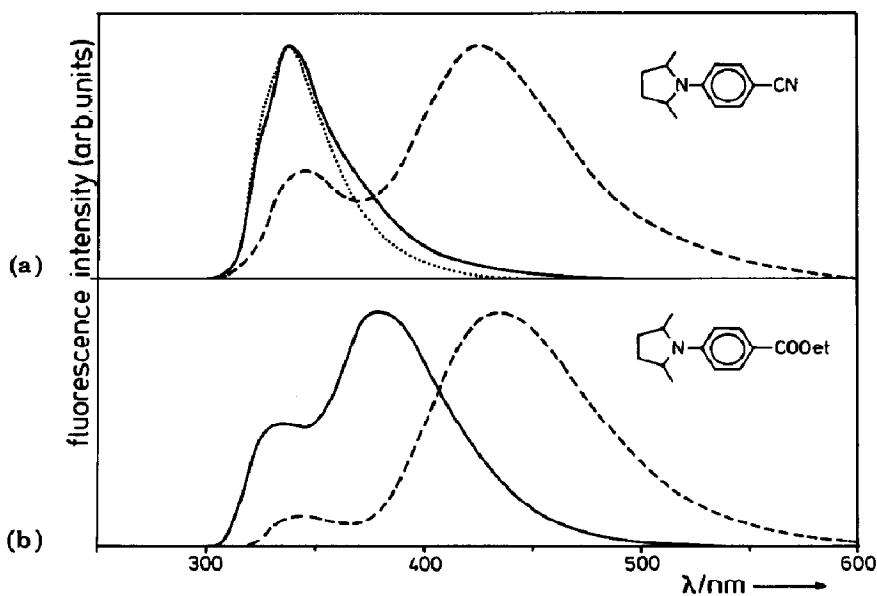


Fig. 2. Fluorescence spectra of (a) compound  $\bar{5D}$  and (b) compound  $\bar{5D}$  in *n*-hexane (—) and *n*-butyl chloride (---) at room temperature; the fluorescence spectrum of compound 1 in *n*-hexane (.....) is shown for comparison.

pound 5 ( $\bar{5}$ ); (iii) the relative TICT yield is larger for the ester series, but the increase for  $\bar{1}$  and  $\bar{5}$  is nearly twice as much as for  $\bar{2}$ ,  $\bar{5D}$  and  $\bar{6}$ ; (iv) since the  $\Phi_A/\Phi_B$  values at 150 K are directly proportional to the rate constant for TICT state formation, the data indicate that  $k$  is fastest for 1 ( $\bar{1}$ ) and 6 ( $\bar{6}$ ) and slowest for 5 ( $\bar{5}$ ) and  $\bar{5D}$  ( $\bar{5D}$ ) (see below).

TABLE 1

$T_{\max}$  and  $\Phi_A/\Phi_B$  at  $T_{\max}$  and 150 K for the nitrile and ester series in the polar solvent *n*-butyl chloride

Compound	$T_{\max}$ (K)	$(\Phi_A/\Phi_B)_{\max}$	$(\Phi_A/\Phi_B)_{150\text{K}}$
<i>Nitrile</i>			
1	196	3	1.2
2	244	9.5	0.62
5	225	0.7	0.12
5D	333	8	0.18
6	183	6.7	3.1
<i>Ester</i>			
1	204	18	5
2	244	25	2.5
5	200	5	1.1
5D	333	22	1.0
6	200	25	5

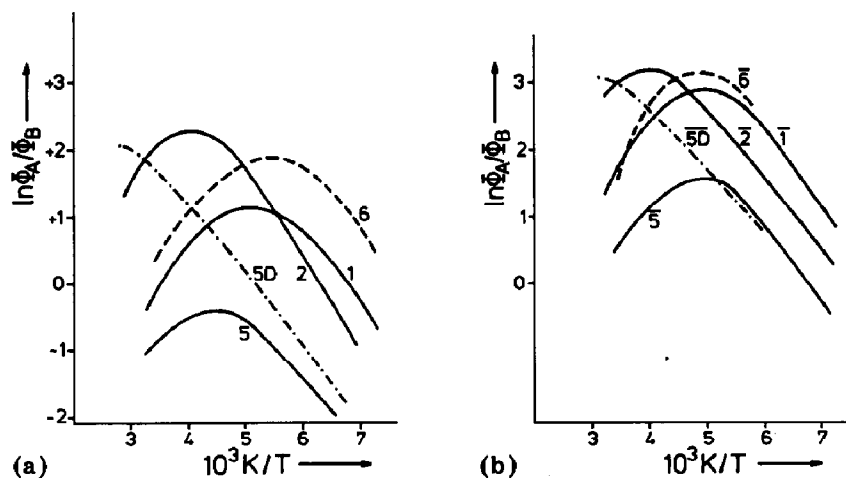


Fig. 3. Temperature dependence of the ratio  $\Phi_A/\Phi_B$  of the long-wavelength to the short-wavelength fluorescence quantum yields of (a) the nitrile and (b) the ester series in *n*-butyl chloride.

Similar data for the dual fluorescence of the ester series in a non-polar hydrocarbon solvent are given in Table 2. It should be noted that  $T_{\max}$  shifts to lower temperatures compared with the polar solvent, and that both  $\Phi_A/\Phi_B$  (max) and  $\Phi_A/\Phi_B$  (150 K) are reduced by a factor of approximately 2 - 13 indicating that the rate constant  $k$  for TICT state formation in non-polar solvents is smaller than that for polar solvents.

For an experimentally independent check, some  $k$  values were directly measured by laser kinetics using the set-up and evaluation procedure de-

TABLE 2

$T_{\max}$  and  $\Phi_A/\Phi_B$  at  $T_{\max}$  and 150 K for the ester series in the non-polar solvent methyl cyclohexane–methyl cyclopentane

Compound	$\bar{1}$	$\bar{2}$	$\bar{5}$	$\bar{5D}$	$\bar{6}$
$T_{\max}^a$ (K)	130	200	—	250	135
$(\Phi_A/\Phi_B)_{\max}$	0.35	6	0.1	4.5	0.37
$(\Phi_A/\Phi_B)_{150\text{ K}}$	0.37	2.2	—	0.45	—

<sup>a</sup>±8 K.

scribed in ref. 11. The  $F_B$  fluorescence decays of the nitrile and ester  $\bar{2}$  and  $\bar{2}$  in the polar solvent at 132 K are compared in Fig. 4. The decay of the ester is so fast ( $\tau_f < 0.2$  ns;  $\bar{k} > 5 \times 10^9$  s<sup>-1</sup>) that the measured decay profile is indistinguishable from the excitation pulse. The B\* state of the nitrile clearly relaxes more slowly, indicating a reduced rate constant ( $\bar{k} \approx 0.24 \times 10^9$  s<sup>-1</sup>).

Laser kinetic measurements were also conducted for the ester  $\bar{2}$  in the non-polar solvent 1:1 methyl cyclohexane–methyl cyclopentane (MCH–MCP) as a function of temperature and yielded values of  $0.5$  ns  $\leq \tau_f \leq 2.5$  ns between 160 and 77 K. The resultant rate constant  $\bar{k}$  obeyed a linear relation on an Arrhenius plot (at least in the temperature range 115–165 K), from which an activation energy of  $7 \pm 2$  kJ mol<sup>-1</sup> was extracted.

The effect of solvent polarity on the rate  $\bar{k}$  of TICT state formation can be evaluated by comparing isoviscous temperatures. The viscosity of *n*-butyl chloride has not been measured at 132 K, but extrapolation of viscosity values determined near room temperature [20] yields an estimated viscosity  $\eta$  of about 15 cP at 132 K (supercooled liquid). MCH–MCP attains this viscosity at 164 K [21], and we find  $\bar{k} \approx 2.2 \times 10^9$  s<sup>-1</sup> for  $\bar{2}$  at this tempera-

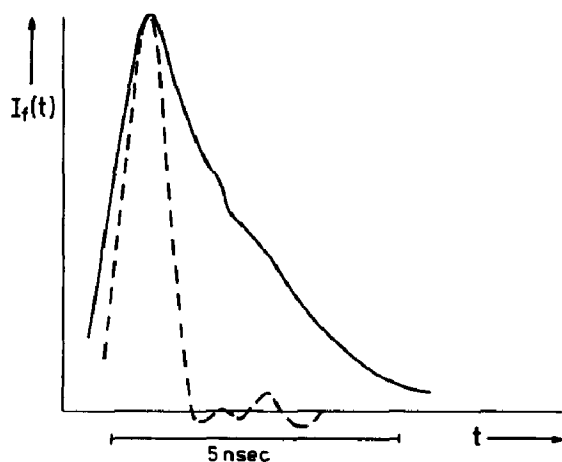


Fig. 4. Decay profile of the short-wavelength fluorescence of the nitrile  $\bar{2}$  (—) and the ester  $\bar{2}$  (---) in *n*-butyl chloride at 132 K. The decay profile of  $\bar{2}$  is indistinguishable from the excitation pulse profile (· · ·).

ture in this solvent. Thus the rate constant  $\bar{k}$  for TICT state formation in  $\bar{2}$  at similar viscosities is accelerated by a factor of more than 2 on increasing the polarity from that of MCH-MCP to that of *n*-butyl chloride.

## 4. Discussion

### 4.1. Thermodynamic versus kinetic control of the formation of twisted intramolecular charge transfer states

It is evident from Figs. 1 and 2 that the esters and nitriles emit a dual fluorescence even in non-polar saturated hydrocarbon (SHC) solvents. Whereas TICT emission is barely detectable in **1** and has only a negligible effect on the halfwidth of the fluorescence band ( $\Delta\nu_{1/2} = 3300 \text{ cm}^{-1}$ ), the corresponding ester **1** shows a sizable fraction of  $F_A$  which increases  $\Delta\nu_{1/2}$  to about  $3700 \text{ cm}^{-1}$ . However, the nitrile **5D** shows a sizable fraction of  $F_A$  already in SHC solvents, and  $F_A$  is the dominant emission from the ester **5D** at room temperature. Other examples which demonstrate that TICT states can be formed in SHC solvents, where specific solute-solvent interactions are unimportant, have been reported in the literature. Both 5,5'-bibenzopyrenyl [22] and 9,9'-bianthryl [23, 24] show dual fluorescence in SHC solvents, and 6-aminocoumarin [25] and twisted derivatives of **1** [26] and 4-cyano-*N*-phenylpyrrole [27] exhibit fluorescence exclusively from the TICT state, even in the gas phase in some cases.

Wermuth [5, 18] has suggested that the greater importance of  $F_A$  for the esters is due to the unusual behaviour of the  $^1L_b$  state. The energy of this state increases on going from nitriles to esters, whereas the energy of the  $^1L_a$  state, which is responsible for the main absorption band, decreases leading to an absorption red shift. Consequently the transition  $B^* \rightarrow \text{TICT}$  in SHC solvents starts from a higher level for the esters and is almost thermoneutral, whereas it is endothermic for the nitriles ( $\Delta H \approx +1000 \text{ cm}^{-1}$  for **1** [5]). The TICT population is thus controlled by thermodynamics. In a similar manner we expect the TICT population of both the nitrile and the ester series to be increased if the energy of the TICT state is slightly reduced. Since the energy of the TICT state is given by the sum of the donor ionization potential  $IP(D)$ , the electron affinity of the acceptor, the Coulomb attraction and the solvent stabilization energy [22], it should directly reflect changes in  $IP(D)$  if all the other factors remain constant. This is indeed found for differently substituted *N*-phenyl pyrroles [28]. These changes are much smaller for the dialkylanilines studied here, but their effect is amplified by the intervention of thermodynamic control. Table 3 gives the donor ionization potentials [10] in decreasing order of magnitude together with the halfwidths of the fluorescence bands of the nitriles and esters in SHC solvents at room temperature. Parallel behaviour is observed, *i.e.* relatively poor donors such as the pyrrolidino or dimethylamino groups are associated with the smallest TICT yields.



TABLE 3

Donor ionization potential IP(D) and halfwidths  $\Delta\nu_{1/2}$  of the fluorescence bands of nitriles and esters in a saturated hydrocarbon solvent at room temperature

Compound	IP(D) (eV)	$\Delta\nu_{1/2}$ ( $\times 10^3 \text{ cm}^{-1}$ )
<i>Nitrile</i>		
1	8.52	3.3
5	8.39	3.4
6	8.28	3.7
2	8.21	3.8
5D	8.17	3.8
<i>Ester</i>		
$\bar{1}$	8.52	3.7
$\bar{5}$	8.39	3.4
$\bar{6}$	8.28	3.9
$\bar{2}$	8.21	5.8
$\bar{5D}$	8.17	6.4 <sup>a</sup>

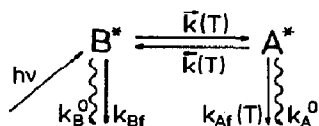
<sup>a</sup>Two bands.

The rate constant  $\vec{k}$  is also thermodynamically controlled for SHC solvents. The values of  $\Phi_A/\Phi_B$  (150 K) in Tables 1 and 2 are, apart from a proportionality constant, a direct measure of  $\vec{k}$  (see below). Since their proportionality constants are similar, the diethylamino (2 and  $\bar{2}$ ) and dimethylamino (1 and  $\bar{1}$ ) compounds can be directly compared. Thus the data in Table 2 indicate that, for the esters in SHC solvents,  $\vec{k}$  for  $\bar{2}$  is a factor of about 6 faster than  $\vec{k}$  for  $\bar{1}$ , which correlates with the increased donor capability of the diethylamino group (Table 3). This is supported by laser kinetic measurements:  $\vec{k}$  is  $7 \times 10^8 \text{ s}^{-1}$  for  $\bar{2}$  in MCH-MCP at 133 K but is only  $2.5 \times 10^8 \text{ s}^{-1}$  for  $\bar{1}$  under the same conditions.

The order of  $\Phi_A/\Phi_B$  (150 K) is reversed in more polar solvents (Table 1), indicating that in both the ester and the nitrile series the TICT state of the dimethylamino compound forms twice as fast as that of the diethylamino compound. This is supported by the results of direct laser kinetic measurements:  $\vec{k}$  is  $3.5 \times 10^8 \text{ s}^{-1}$  for 2 in *n*-butyl chloride at 138 K and increases to  $10 \times 10^8 \text{ s}^{-1}$  for 1 under the same conditions. Thus in polar solvents, where the TICT state lies well below the B\* state,  $\vec{k}$  ceases to be thermodynamically controlled and diffusion kinetic control takes over. This can lead to rate constant reversals as shown above because many additional factors such as molecular flexibility, rotator size and free-volume effects become important [10, 11].

#### 4.2. Kinetic consequences of an avoided crossing

The following simple kinetic scheme proposed by Grabowski and co-workers [2] is used for the kinetic analysis of the quantum yield data in Tables 1 and 2:



In the low temperature region the quantum yields for  $F_A$  and  $F_B$  and their ratio are given by [19]

$$\Phi_A = \frac{\bar{k}k_{Af}}{(k_{Af} + k_A^0)(\bar{k} + k_{Bf} + k_B^0)} \quad (2)$$

$$\Phi_B = \frac{k_{Bf}}{\bar{k} + k_{Bf} + k_B^0} \quad (3)$$

$$\frac{\Phi_A}{\Phi_B} = \frac{\bar{k}k_{Af}}{k_{Bf}(k_{Af} + k_A^0)} \quad (4)$$

Thus  $\Phi_A/\Phi_B$  yields directly the ratio  $\bar{k}/k_{Bf}$  multiplied by a factor  $k_{Af}/(k_{Af} + k_A^0)$  which corresponds to the intrinsic fluorescence quantum yield  $\Phi_A^{\text{intr}}$  of the TICT state. Because of the forbidden nature of the TICT state,  $\Phi_A^{\text{intr}}$  is small (0.033) for the nitriles 1, 2 and 6 in *n*-butyl chloride [10]. It is even smaller (0.011) for the pyrrolidino compounds 5 and 5D because they are less flexible and possess a narrower angular distribution function around the perpendicular TICT geometry [10]. A similar value of about 2.3 for the ratio of  $\Phi_A^{\text{intr}}$  of compounds 1 and 2 to  $\Phi_A^{\text{intr}}$  of the pyrrolidino compound 5D is found for the ester series in SHC solvents ( $\Phi_A^{\text{intr}}$  has values of 0.087 and 0.039 respectively). The corresponding values for the esters in *n*-butyl chloride are 0.065 and 0.025. The non-radiative decay constant  $k_A^0$  of the TICT state seems to be more important for nitriles than for esters, possibly because of acceleration of the intersystem crossing pathway by the cyano group [7]. However, it is still not clear whether the main TICT deactivation occurs via intersystem crossing or via internal conversion. The values of  $\bar{k}$  are derived from the  $k_{Bf}$  values for the nitriles and esters ( $7.7 \times 10^7 \text{ s}^{-1}$  and  $25 \times 10^7 \text{ s}^{-1}$  respectively), which are accessible from the limiting low temperature fluorescence decay rate and quantum yield data [18] and are associated with the transition moment from the  $^1L_b$  and  $^1L_a$  states respectively. They are given in Table 4.

As mentioned above, TICT state formation is much faster for the esters than for the nitriles, e.g. by factors of 2.6 - 13 in *n*-butyl chloride. We also expect the esters to react faster at room temperature. A value of 10 ps has recently been reported for the  $\bar{k}$  of DMABN in acetonitrile at room temperature [29]; this is much slower than the dielectric relaxation time of this solvent (1 ps) [30]. Thus  $\bar{k}$  for the corresponding ester 1 can be expected to compete with the dielectric relaxation time; in the light of recent discussions by Kosower [31] this would be an interesting subject for picosecond investigations.

TABLE 4

Mean Franck-Condon twist angles ( $\varphi_{FC}$ ) and rate constants for TICT formation determined for nitriles and esters in *n*-butyl chloride at 150 K using eqns. (1) and (4)

Compound	$\varphi_{FC}^a$ (deg)	$\vec{k}$ ( $\times 10^9 \text{ s}^{-1}$ )
<i>Nitrile</i>		
5	0	0.84
1	4	2.8
5D	10	1.3
2	21	1.5
6	33	7.2
<i>Ester</i>		
5		11.0
1		19.2
5D		10.0
2		9.6
6		19.2

<sup>a</sup>From ref. 12.

Apart from this increase in  $\vec{k}$  which is responsible for the upward shift of the  $\ln(\Phi_A/\Phi_B)$  curves in Fig. 3, there is little additional change in the gross features of this figure. The equilibration temperatures  $T_{\max}$ , the low temperature slopes and the order of the maximum  $\Phi_A/\Phi_B$  values are unchanged in going from nitriles to esters. This signifies that the same rate-determining factors (kinetic control as discussed above) must be active; the main difference is the absence of conical intersections along the reaction coordinate in the case of the esters. This seems to affect the pre-exponential factor of  $\vec{k}$  but not its activation energy.

Figure 5 shows a schematic representation of the relevant region of the hypersurface. In this region the two states with different symmetry representations ( ${}^1L_a$  and  ${}^1L_b$ ) approach each other very closely and interact vibronically via an asymmetric vibration. The adiabatic potential along the asymmetric normal mode  $q_n$  is thus transformed into a diabatic double-minimum potential on the lower surface [8]. This results in an upward-directed cone on the lower hypersurface and a downward-directed cone on the upper hypersurface centred at the crossing point where the twist angle has the critical value  $\varphi_{cr}$  (Fig. 5(a)). This is known as a conical intersection [32] and hypersurface topologies of this type are also important in discussions of photoelectron spectra [32] and the depopulation kinetics of excited states [33].

The critical twist angle  $\varphi_{cr}$  depends on the relative energies of the  $B^*$  and  $A^*$  states. The  $A^*$  state, which is more polar, responds more strongly to changes in the solvent surrounding. Thus  $\varphi_{cr}$  is expected to move to lower values in more polar solvents. If the  $A^*$  state is sufficiently stable or the  $B^*$  state is shifted upwards, as in the esters [18], the crossing is removed and  $\varphi_{cr}$  vanishes altogether (Fig. 5(b)). Then  $F_A$  and  $F_B$  are expected to show

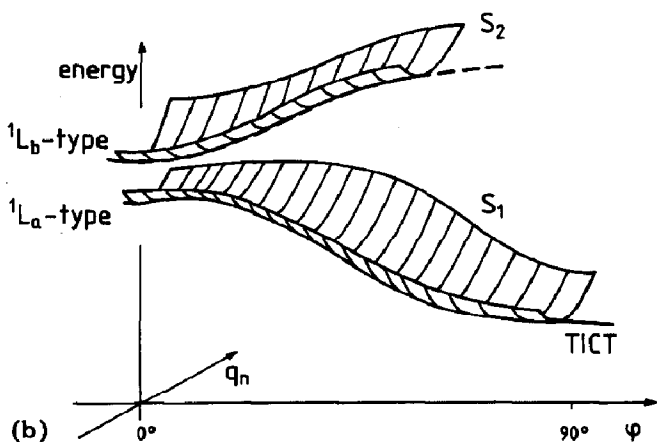
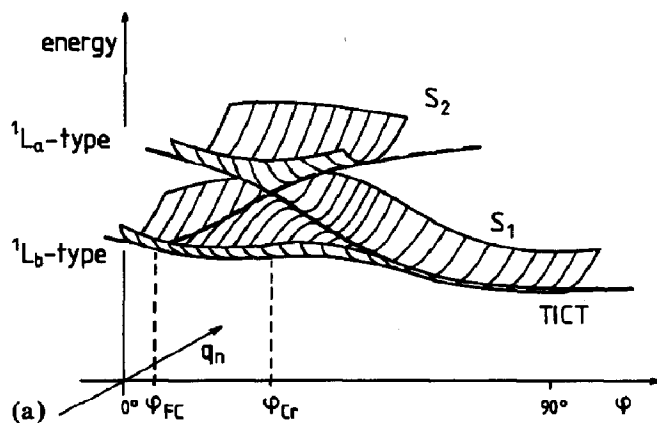


Fig. 5. (a) Schematic representation of a conical intersection along the reaction coordinate towards the TICT state in the nitrile series; (b) similar diagram for the ester series where a different state correlation exists and the conical intersection is absent (the existence of the small barrier separating the B\* and A\* (TICT) states is hypothetical and has not yet been established).

equal fluorescence polarization, as is found for the esters [7]. The early polarization data reported by Rotkiewicz *et al.* [34] for DMABN in glycerol (both bands show a large positive polarization) can also be interpreted as indicating state reversal in this solvent because they contrast strongly with the polarization data in ethanol at low temperatures [7]. A similar solvent-induced state reversal has been observed for a naphthyl analogue of DMABN [35].

It has been shown [12] that the mean ground state twist angle, which is equal to the mean Franck-Condon twist angle ( $\langle\varphi_{FC}\rangle$ ) (see Table 4) is one of the main factors determining the pre-exponential term of  $\bar{k}$ . Pretwisted compounds with hindered planarity adopt the TICT geometry more rapidly (*e.g.* compounds 5D and 6 compared with compounds 5 and 2). The reason for this is obvious from Fig. 5(a). If  $\varphi_{FC}$  is on the left-hand side of  $\varphi_{cr}$  (unhindered or only slightly hindered planarity), the region between  $\varphi_{FC}$  and

$\varphi_{cr}$  corresponds to an energetically flat region which has to be crossed in order to reach the TICT state by "surrounding" the cone at  $\varphi_{cr}$ . As there is little or no driving force, this gap is transversed comparatively slowly in a motion similar to an angular diffusion process without driving force. The driving force is strongly increased for angles between  $\varphi_{cr}$  and  $90^\circ$  or along the whole reaction coordinate in Fig. 5(b). This differing dependence of the driving forces on the reaction coordinate seems to be the source of the difference between the rate constants (difference between the  $A$  factors) observed for esters and nitriles. For more polar solvents, where  $|\varphi_{FC} - \varphi_{cr}|$  is reduced in the nitrile series, the pre-exponential factor of  $\vec{k}$  is expected to increase leading to a solvent-polarity-dependent rate of TICT state formation. This has recently been observed for DMABN [36].

#### 4.3. Free-volume effects

The low temperature slopes of  $\ln(\Phi_A/\Phi_B)$  versus  $1/T$  (Fig. 3), which yield the value for the activation energy  $\vec{E}$  of  $\vec{k}$  [19], are all very similar, and  $\vec{E}$  is significantly below the activation energy of  $E_\eta$  of the macroscopic solvent viscosity  $\eta$  [1]. It is surprising that nitriles and esters should exhibit the same slope because the shapes of their hypersurfaces are very different.  $\vec{E}$  can be interpreted as being a very complex combination of (i) a (static) barrier in the potential surface (as indicated in Fig. 5(b)) and (ii) a barrier induced dynamically by the effect of viscous flow as described by Dellinger and Kasha [37]. If (ii) is the major contribution  $\vec{E}$  will cease to depend on the driving force, and free-volume effects are likely to become important. Some evidence for this has been obtained by direct measurement of the temperature dependence of  $\vec{k}$  for the nitrile series where the reduced  $\vec{E}$  values of certain symmetric compounds were interpreted as being indicative of a large fraction of rotational diffusion into the available free volume [11]. It is also possible that the "magic" exponent  $2/3$  found by Förster and Hoffmann [38] for the dependence of the fluorescence quantum yield of triphenyl methane (TPM) dyes on the solvent viscosity  $\eta$  has the same source. There is now kinetic evidence that TPM dyes relax towards a low-lying non-fluorescent TICT-like state with twisted conformation and charge localization [39]. Since the dependence  $\Phi_f = C\eta^{2/3}$  is equivalent to  $\vec{E} = \frac{2}{3}E_\eta$  [11], it is possible that this value constitutes a limiting dynamic barrier for the rotation of a phenyl or aniline rotor under the action of driving forces above a certain threshold. These rotors are almost symmetric and should relax into the available free volume with little hinderance.

The pyrrolidino group in 5, which shows the lowest  $\vec{E}$  value, is a similar symmetric rotor. Larger asymmetric groups like dimethylpiperidino lead to increased  $\vec{E}$  values which are indicative of reduced free-volume effects [11]. A limiting case seems to be the intramolecular excimer formation of  $\alpha,\omega$ -biarylalkanes where the dependence found is proportional to  $\eta^1$  [40]. This may be the consequence of a very small driving force and of the large size of the aromatic groups which make it very unlikely that their diffusion takes place by the occupation of the solvent free volume.

When Fig. 3 and Tables 1 and 2 are inspected more closely several subtle differences emerge.

(i) The order of  $\Phi_A/\Phi_B$  in the low temperature region is  $5D > 5$  for the nitriles but  $5\bar{D} < \bar{5}$  for the esters.

(ii) The difference between 1 and 6 varies in the same sense: 6 approaches the TICT state more rapidly than 1 does for the nitriles, but  $\bar{1}$  shows approximately the same rate as  $\bar{6}$  for the esters.

(iii) The quantitative changes which occur on going from the nitriles to the esters are most readily revealed by comparing the  $(\Phi_A/\Phi_B)_{\max}$  values. The compounds studied fall into two groups: for  $\bar{2}$  (2),  $5\bar{D}$  (5D) and  $\bar{6}$  (6) the values for the ester are increased by a factor of 2.5 - 3.7, whereas for  $\bar{1}$  (1) and  $\bar{5}$  (5) they increase by a factor of about 6 - 7. These differences may be due to the following reasons. The disappearance of the conical intersection on going from nitriles to esters should have a particularly strong effect for those nitrile compounds with a large gap  $|\varphi_{FC} - \varphi_{cr}|$  such as the near-planar compounds 1 and 5 [12]. The difference between the two groups is expected to become smaller for more polar solvents where  $|\varphi_{FC} - \varphi_{cr}|$  is reduced. In addition 1 and 5 are both symmetrical compounds which can be expected to relax easily by rotational diffusion into the available free volume. It is thus reasonable to expect these compounds to respond particularly strongly to changes in the driving force along the reaction coordinate.

Some other effects in the dual fluorescence of nitriles and esters which are due to occupation of the free volume of the solvent are readily observable even at room temperature. 1 shows different high temperature  $\Phi_A/\Phi_B$  ratios for cyclic (MCH-MCP or decaline) and acyclic (3-methylpentane) alkane solvents [5]. This can be explained by (i) taking into account the larger polarizability of cyclic alkanes and (ii) assuming that more free volume is available in the cyclic alkanes. The dual fluorescence of DMABN and related molecules has also been observed in poly(methyl methacrylate) [41], poly(vinyl alcohol) and nylon [42] rigid matrices. This suggests that DMABN and related TICT-forming molecules may be suitable probes for sensing the free volumes and microvoids in polymers of various structures and textures. A particularly striking example of the use of the free volume is the formation of the TICT state in 6-aminocoumarin [25] which is observed even in an ethanol matrix at 77 K. Even that environment seems to contain voids which are large enough to allow rotation of the amino group.

### Acknowledgments

The authors are grateful to Professor E. Lippert for discussions and encouragement. W.R. wishes to thank Mrs. Barbara Dewald for recording the low temperature fluorescence spectra. Financial support by the Deutsche Forschungsgemeinschaft and the Fonds der Chemischen Industrie is gratefully acknowledged. Part of the work was done under project 05286 Li I of the Bundesministerium für Forschung und Technologie.

## References

- 1 E. Lippert, W. Lüder and H. Boos, in A. Mangini (ed.), *Advances in Molecular Spectroscopy*, Pergamon, Oxford, 1962, p. 443.
- 2 Z. R. Grabowski, K. Rotkiewicz, W. Rubaszewska and E. Kirkor-Kaminska, *Acta Phys. Pol. A*, **54** (1978) 793.  
S. Dähne, W. Freyer, K. Teuchner, J. Dobkowski and Z. R. Grabowski, *J. Lumin.*, **22** (1980) 37.  
J. Dobkowski, E. Kirkor-Kaminska, J. Koput and A. Siemiarczuk, *J. Lumin.*, **27** (1982) 339.
- 3 W. Rettig and E. A. Chandross, submitted to *J. Am. Chem. Soc.*
- 4 G. Wermuth, W. Rettig and E. Lippert, *Ber. Bunsenges. Phys. Chem.*, **85** (1981) 64.
- 5 G. Wermuth, *Z. Naturforsch., Teil A*, **38** (1983) 641.
- 6 Z. R. Grabowski, K. Rotkiewicz, A. Siemiarczuk, D. J. Cowley and W. Baumann, *Nouv. J. Chim.*, **3** (1979) 443.
- 7 W. Rettig, G. Wermuth and E. Lippert, *Ber. Bunsenges. Phys. Chem.*, **83** (1979) 692.
- 8 G. Wermuth and W. Rettig, *J. Phys. Chem.*, **88** (1984) 2729.
- 9 E. Lippert, A. A. Ayuk, W. Rettig and G. Wermuth, *J. Photochem.*, **17** (1981) 237.
- 10 W. Rettig, *J. Lumin.*, **26** (1981) 21.
- 11 W. Rettig, *J. Phys. Chem.*, **86** (1982) 1970.
- 12 W. Rettig and R. Gleiter, submitted to *J. Phys. Chem.*
- 13 R. J. Visser and C. A. G. O. Varma, *J. Chem. Soc., Faraday Trans. II*, **76** (1980) 453.
- 14 R. J. Visser, C. A. G. O. Varma, J. Konijnenberg and P. Bergwerf, *J. Chem. Soc., Faraday Trans. II*, **79** (1983) 347.
- 15 R. J. Visser, P. Weisenborn and C. A. G. O. Varma, *Chem. Phys. Lett.*, **113** (1985) 330.
- 16 G. Wermuth, *Ph.D. Dissertation*, Technical University, Berlin, 1982.
- 17 H. Suhr, *Justus Liebigs Ann. Chem.*, **687** (1965) 182.
- 18 G. Wermuth, *Z. Naturforsch., Teil A*, **38** (1983) 368.
- 19 W. Rettig and E. Lippert, *J. Mol. Struct.*, **61** (1980) 17.
- 20 J. A. Riddick and W. B. Bunger, *Techniques of Chemistry*, Vol. II, *Organic Solvents*, Wiley-Interscience, New York, 3rd edn., 1970, p. 339.
- 21 G. A. von Salis and H. Labhart, *J. Phys. Chem.*, **72** (1968) 752.
- 22 M. Zander and W. Rettig, *Chem. Phys. Lett.*, **110** (1984) 602.
- 23 R. J. Visser, P. C. M. Weisenborn, P. J. M. van Kan, B. H. Huizer, C. A. G. O. Varma, J. M. Warman and M. P. de Haas, *J. Chem. Soc., Faraday Trans. II*, to be published.
- 24 W. Baumann and R. J. Visser, cited in W. Rettig, Report on the Workshop on the nature of the so-called TICT states, *EPA Newsletters*, July 1984, p. 25.
- 25 W. Rettig and A. Klock, *Can J. Chem.*, to be published.
- 26 K. Rotkiewicz and W. Rubaszewska, *J. Lumin.*, **27** (1982) 221.  
K. Rotkiewicz and W. Rubaszewska, *Chem. Phys. Lett.*, **70** (1980) 444.
- 27 W. Rettig, Report on the workshop on the nature of the so-called TICT states, *EPA Newsletters*, July 1984, p. 25.
- 28 W. Rettig and F. Marschner, *Nouv. J. Chim.*, **7** (1983) 425.
- 29 K. Rotkiewicz, Z. R. Grabowski and J. Jasny, *Chem. Phys. Lett.*, **34** (1975) 55.  
D. Huppert, S. D. Rand, P. M. Rentzepis, P. F. Barbara, W. S. Struve and Z. R. Grabowski, *J. Chem. Phys.*, **75** (1981) 5714.  
Y. Wang, M. McAuliffe, F. Novak and K. B. Eisenthal, *J. Phys. Chem.*, **85** (1981) 3736.
- 30 J. E. Griffiths, *J. Chem. Phys.*, **59** (1973) 751.
- 31 E. M. Kosower, *Acc. Chem. Res.*, **15** (1982) 259.
- 32 H. Köppel, L. S. Cederbaum, W. Domcke and S. S. Shaik, *Angew. Chem.*, **95** (1983) 221.  
H. Köppel, W. Domcke and L. S. Cederbaum, *Adv. Chem. Phys.*, **57** (1984) 59.

- 33 A. J. Lorquet, J. C. Lorquet, J. Delwiche and M. J. Hubin-Franskin, *J. Chem. Phys.*, **76** (1982) 4692.
- 34 K. Rotkiewicz, K. H. Grellmann and Z. R. Grabowski, *Chem. Phys. Lett.*, **19** (1973) 315; **21** (1973) 212.
- 35 A. A. Ayuk, W. Rettig and E. Lippert, *Ber. Bunsenges. Phys. Chem.*, **85** (1981) 553.
- 36 J. Hicks, cited by W. Rettig, Report on the workshop on the nature of the so-called TICT states, *EPA Newsletters*, July 1984, p. 25.
- 37 B. Dellinger and M. Kasha, *Chem. Phys. Lett.*, **36** (1975) 410.
- 38 Th. Förster and G. Hoffmann, *Z. Phys. Chem. N.F.*, **75** (1971) 63.
- 39 M. Vogel and W. Rettig, *Proc. 10th IUPAC Symp. on Photochemistry, Interlaken, July 1984*, Presses Polytechniques Romandes, Lausanne, p. 579.
- 40 H. Staerk, R. Mitzkus, W. Kühnle and A. Weller, in K. B. Eisenthal, R. M. Hochstrasser, W. Kaiser and A. Laubereau (eds.), *Picosecond Phenomena*, Vol. 3, Springer, Berlin, 1982, p. 205.
- 41 K. Al-Hassan and W. Rettig, unpublished results, 1984.
- 42 C. Cazeau-Dubroca, A. Peirigua, S. Ait Lyazidi and G. Nouchi, *Chem. Phys. Lett.*, **98** (1983) 511.